Journal of Integrative Agriculture 2026, 25(7): 2723–2738

Available online at ScienceDirect

Journal of Integrative Agriculture



RESEARCH ARTICLE

A genome-wide association study integrated with transcriptome analysis to identify boron efficiency-related candidate genes and favorable haplotypes in *Brassica napus* L.

Ziwei Zhang[1, 2], Haoqiang Zhai[3], Yingpeng Hua[4], Sheliang Wang[2], Fangsen Xu[1, 2#]

[1] *National Key Laboratory of Crop Genetic Improvement, Huazhong Agricultural University, Wuhan 430070, China*
[2] *Microelement Research Center, College of Resources & Environment, Huazhong Agricultural University, Wuhan 430070, China*
[3] *Hubei Yishizhuang Agricultural Technology Co., Ltd., Yichang 443000, China*
[4] *School of Agricultural Sciences, Zhengzhou University, Zhengzhou 450001, China*

Highlights

- A natural population of *Brassica napus* with 391 accessions was employed to identify boron (B) efficiency-related beneficial alleles with genome-wide association study (GWAS).
- *BnaA03g29020D*, *BnaA03g29440D*, *BnaC03g33010D*, and *BnaC03g34490D* were identified as candidate genes potentially involved in the efficient utilization of B in *B. napus*.
- The favorable haplotypes had better seedling growth and productivity within the rapeseed population under B deficiency conditions.

Abstract

Rapeseed (*Brassica napus* L.) is a major oil crop worldwide that is vigorously promoted for cultivation in China. Boron (B) is an essential micronutrient for plant growth and development. However, the agricultural soils in rapeseed planting areas often show either B deficiency or severe B deficiency. Increasing the resistance to B deficiency is a pivotal goal in the breeding of rapeseed, yet the genetic basis for variations in B efficiency-related traits remains unclear. In this study, a natural population with 391 rapeseed accessions and a nutrient solution system were used to investigate B efficiency-related traits, including relative root length (RRL), shoot dry weight (SDW), root dry weight (RDW), and B efficiency coefficient (BEC), all of which exhibited extensive phenotypic variations under B deficiency. Through a genome-wide association study (GWAS) of B efficiency-related traits using high-density SNP markers obtained from whole-genome resequencing, 106 significantly associated SNPs were identified by employing both the general linear model and the mixed linear model. Among these SNP loci, two prominent SNP clusters were detected on chrA03: 14,087,835–14,764,672 and chrC03: 20,110,319–22,135,492 at low B levels across three repeated experiments of multiple traits. Integrating those results with a transcriptome analysis, four genes exhibiting higher differentially expressed fold-change along with favorable haplotypes within the promoter or coding region, *BnaA03g29020D*, *BnaA03g29440D*, *BnaC03g33010D*, and *BnaC03g34490D*, were identified as candidate genes that could potentially be involved in efficient B utilization, and their favorable haplotypes were found to improve seedling growth and productivity under B deficiency. Considering the lack of B mineral resources in China, the rapid and accurate identification of more B-efficient alleles and studying the genetic mechanism underlying crop responses to B deficiency have important theoretical and practical significance for cultivating B-efficient varieties and maintaining green, sustainable agriculture.

Keywords: rapeseed, boron deficiency, GWAS, transcriptomic analysis, favorable haplotypes, B efficiency

Received 25 June 2024; Received in revised form 4 September 2024; Accepted 24 September 2024; Available online 5 November 2024
#Correspondences Fangsen Xu, E-mail: fangsenxu@mail.hzau.edu.cn

© 2026 CAAS. Publishing services by Elsevier B.V. on behalf of KeAi Communications Co. Ltd. This is an open access article under the CC BY-NC-ND license (http://creativecommons.org/licenses/by-nc-nd/4.0/). Peer review under responsibility of Editorial Board of *Journal of Integrative Agriculture*.
doi: 10.1016/j.jia.2024.11.013

1. Introduction

Boron (B) is a crucial microelement for plant growth and development (Warington 1923). Due to the restricted availability of B in soil, B deficiency is a global issue affecting agriculture production that has been documented in more than 80 countries across various regions (Tanaka and Fujiwara 2008). The primary role of B is to cross-link pectic rhamnogalacturonan II (RG-II), which helps to establish and maintain the structural integrity of plant cell walls (Begum and Fry 2022). In plants, symptoms of B deficiency primarily manifest in the growing and expanding organs across the entire plant. Both root elongation and leaf expansion are inhibited in B deficiency. In addition, B deficiency also inhibits flower development and seed setting (Takano *et al.* 2006; Tanaka *et al.* 2008; Onuh and Miwa 2021). Thus, B deficiency causes reductions in crop yield and quality. As B is not efficiently remobilized from mature to developing organs, plants must obtain a continuous supply of B and transport it to growing tissues for efficient agricultural production (Brown and Shelp 1997). Rapeseed (*Brassica napus* L.) is an important oilseed crop that provides approximately 13% of global edible oil production (USDA and ERS 2024). *Brassica napus* is one of the *Brassica* species that has a high B requirement and is quite sensitive to B deficiency (Zhang *et al.* 2014b). "Flowering without seed setting" is widely recognized as a common severe symptom of B deficiency in *B. napus* and is now considered to be a leading threat to rapeseed production (Wang *et al.* 2007). In recent decades, the application of B fertilizers has been implemented in agricultural practices to address this problem (Wang *et al.* 2007). Nevertheless, B has the narrowest range of soil concentrations between deficiency and toxicity among all the essential mineral elements (Camacho-Cristóbal *et al.* 2008). As an essential microelement in plants, boron can be toxic in excessive concentrations, and excess B can accumulate in mature tissues, which may also have detrimental effects on crop yield. Therefore, enhancing the genetic improvements for efficient B use is a desirable strategy to increase crop productivity in B-deficient regions or crops sensitive to B deficiency.

In the last two decades, genetic studies have shown that the absorption and transport of B in plants are regulated by two distinct types of membrane proteins. One type is known as NOD26-like intrinsic proteins (NIPs), which function as membrane channel proteins and help facilitate boric acid permeation. The other type is borate exporters (BORs), which are transporters that export borate from cells (Onuh and Miwa 2021). In recent years, the quantitative trait locus (QTL) *qBEC-A3a* controlling the B efficiency coefficient (BEC) of *B. napus* was characterized using a double haploid (DH) population generated by crossing Qingyou 10 (QY10, B efficient) with Westar10 (W10, B inefficient), which can explain 30.79% of the phenotypic variance (Zhang *et al.* 2014a). Subsequently, a major effect QTLs analysis using fine-scale mapping combined with digital gene expression (DGE) profiling revealed that B efficiency-targeted *BnaA3*. *NIP5;1* is the candidate gene for *qBEC-A3a*. The expression level of *BnaA3*. *NIP5;1* was found to be markedly elevated in QY10 roots compared to W10, hence contributing to the observed low B tolerance in QY10 (Hua *et al.* 2016a). Traditional rapeseed mapping studies have identified some loci associated with B efficiency-related traits (Zhang *et al.* 2014a), but only a few have successfully identified the underlying genes within the detected QTLs. The further fine mapping of QTLs to narrower and more precise genetic intervals and the subsequent cloning of the underlying genes are notably resource- and time-intensive efforts, which often require the establishment of large secondary populations to attain sufficient map resolution (Dinka *et al.* 2007). While biparental QTL mapping is effective for uncovering underlying genes, its ability to describe allelic diversity and genomic resolution is limited. In contrast, genome-wide association studies (GWAS) offer advantages over traditional methods due to high resolution and the identification of allelic variants (Prince *et al.* 2019).

Developments in bioinformatics and genome-sequencing technology have made the genetic analysis of complex crop traits achievable (Lu *et al.* 2019). In recent years, performing GWAS using single-nucleotide polymorphisms (SNPs) across large numbers of individual genomes has been an effective approach for identifying potential candidate genes and/or genetic regions that control significant agronomic traits in many field crops (Wu *et al.* 2019). Previous studies on rapeseed have used GWAS to dissect traits such as root architecture (Yuan *et al.* 2023), flowering time (Huang *et al.* 2021), seed yield (Pal *et al.* 2021), seed quality (Körber *et al.* 2016), and harvest index (Lu *et al.* 2016). However, to date, there has been no documented genome-wide association mapping of B efficiency-related genes in *B. napus*. Natural hybridization between *B. rapa* (AA, 2n=20) and *B. oleracea* (CC, 2n=18) produced *B. napus* (AACC, 2n=38), resulting in great genetic potential for extensive phenotypic variation (Hu *et al.* 2022). Thus, conducting GWAS on B efficiency-related traits is essential for obtaining comprehensive knowledge of the genetic foundations and molecular mechanisms that are responsible for B uptake and transport in the *B. napus* population.

In a previous study, Tang *et al.* (2021) sequenced a collection of 505 *B. napus* accessions to explore its genetic diversity, which was used in this study. Here, we quantified the relative root length (RRL), shoot dry weight (SDW), root dry weight (RDW), and BEC of 391 rapeseed accessions using a hydroponic system. These parameters are known to be reliable indicators of plant growth in the presence of B deficiency (Zhang *et al.* 2014a). Moreover, quantitative inheritance of these important traits has been attributed to polygenes and gene-environment interactions (Xiao *et al.* 2017). Those four traits under different B treatments were then used to perform GWAS to detect genes potentially related to B efficiency. This study is the first to use the GWAS approach to identify candidate genes related to B efficiency in rapeseed. Our results provide valuable insights into the genetic basis underlying B efficiency-related traits and will facilitate rapeseed genetic improvement in the future.

2. Materials and methods

2.1. Plant materials

The natural association population consisted of 391 accessions, with 356 lines originating from China, 20 from Europe, five from Canada, one from America, three from Australia, four from Korea, and two from Japan. The accessions were gathered from major breeding facilities across China, comprising 284 semi-winter, 70 winter, 34 spring, and three undetermined types (Tang *et al.* 2021) (Appendix A).

2.2. Phenotyping of B efficiency-related traits and statistical analysis

The B efficiency-related traits of the natural population were determined by treating the plants at low B (LB: 0.25 μmol L^{-1} B) and normal B (NB: 25 μmol L^{-1} B) levels using a modified standard Hoagland's solution (Appendix B). Plump seeds of a similar size were sterilized using 75% (v/v) ethanol and NaClO (2.5% active chlorine) and then germinated with ultra-pure water (18.25 MΩ) on gauze for 5 days. The uniformly grown seedlings were then transplanted to hydroponic growth tanks and cultured with a 50% standard Hoagland's solution for the first 5 days, followed by 100% standard Hoagland's solution for the next 10 days. The nutrient solution was changed every 5 days. The seedlings were cultivated in an illuminated growth chamber at 22°C under a 16 h light/8 h dark cycle. The photosynthetic photon flux density was 300–320 mmol m^{-2} s^{-1}, and the relative humidity was 60–75%. The primary RRL was measured using a ruler when the seedlings were transplanted into the hydroponic growth tank and when the seedlings were collected after 15 days, and then the RRL (RRL=$RRL_{15\ d}$–$RRL_{0\ d}$) was calculated. Seedling samples were dried at 65°C for 3 days until a constant weight was obtained and the dry weight was measured. The BEC was used to evaluate the B efficiency of the cultivars, which is the ratio of a plant's dry weights under LB and NB conditions. The different B treatments were repeated three times, with six biological replicates for each variety every time.

The B efficiency-related trait phenotypes were statistically analyzed using Microsoft Excel 2007 software, which included calculating the average value (mean), standard deviation (SD), maximum (Max), minimum (Min), coefficient of variation (CV%), and Kolmogorov-Smirnov test (*P*). The R packages "ggplot2" (https://cran.r-project.org/web/packages/ggplot2/index.html), "corrplot", "Hmisc" (https://rdrr.io/cran/Hmisc/), and "Psych" (https://CRAN.R-project.org/package=psych) were used to analyze the phenotypic distributions and correlations. The best linear unbiased prediction (BLUP) values of the four B efficiency-related traits for each accession were calculated by R package 'lme4' (Piepho *et al.* 2003). The BLUP values were subsequently used as phenotypic data for the GWAS. The broad-sense heritability (H^2) was calculated according to the formula: $h^2=\sigma^2_G/(\sigma^2_G+\sigma^2_{GE}/e+\sigma_e^2/re)$, where σ^2_G is genetic variation, σ^2_{GE} is the interaction variance between genotype and environment, σ_e^2 is residual variance, e is the number of environments, and r is the number of repeats in each environment.

2.3. Population structure, relative kinship, and linkage disequilibrium analysis

A total of 1,507,767 high-quality SNPs with minor allele frequency (MAF)>0.05 and missing rates<0.2 were used for the GWAS in this study (Tang *et al.* 2021). Population structure and kinship were employed to correct for any spurious associations resulting from genotype-phenotype covariance. The population structure was assessed using Admixture software (Alexander *et al.* 2009). Tassel 5.0 software was used to calculate the relative kinship matrix, which shows the genetic relatedness between samples (Bradbury *et al.* 2007; http://www.maizegenetics.net/tassel). The linkage disequilibrium (LD) statistic R^2 between the SNPs was calculated using PopLDdecay software (Zhang *et al.* 2019).

2.4. Genome-wide association analysis of the B efficiency-related traits

This study used Tassel 5.0 software to conduct the GWAS for four B efficiency-related traits using both general linear models (GLMs) and mixed linear models (MLMs). Fixed effects were estimated using a Q (population structure) matrix and random effects using a Kinship (K) matrix. The MLM considered Q+K matrices, while the GLM only considered a Q matrix (Bradbury *et al.* 2007). The *P*-value of each SNP was calculated and the suggestive *P*-value (1/*n*) was used as a cutoff. The Manhattan and quantile-quantile plots (Q-Q plot) were created with $-\log_{10}P$ observed and expected values using the R package ggplot2 and CMplot (https://cran.rproject.org/web/packages/CMplot), respectively.

2.5. Transcriptome analysis and identification of differentially expressed genes (DEGs)

Based on the previously reported genome-wide transcriptomic responses of rapeseed to B deficiency (Hua *et al.* 2017), the sequencing data of boron sufficient leaves (BsL), boron deficient leaves (BdL), boron sufficient roots (BsR), and boron deficient roots (BdR) were selected to analyze the DEGs responding to different B treatments. This transcriptome analysis employed 'Westar10' (W10) to identify the transcriptomic responses to B deficiency in the leaves and roots of 'W10' seedlings cultivated under B deficiency (0.25 μmol L^{-1}) and B sufficiency (25 μmol L^{-1}) conditions for 10 days. In addition, the DGE profiling of different rapeseed genotypes responding to B deficiency was also analyzed (Hua *et al.* 2016b). The DGE profiling was performed on the leaves and roots of 'QY10' and 'W10' seedlings that were treated with B deficiency (0.25 μmol L^{-1}) for 10 days. This study employed false discovery rate (FDR)≤0.05 and the absolute value of $\log_2$(fold-change)≥1 as the DEG screening thresholds.

2.6. Prediction of candidate genes

According to the LD distance of the chromosome where the significant SNPs identified by the association analysis are located, the genes within the LD distance on both sides of the target SNP were initially regarded as candidate genes. For further candidate gene identification, the 300 kb flanking

regions upstream and downstream of significantly associated SNPs were used as confidence intervals. In order to identify candidate genes that control B efficiency-related traits, the GWAS results were integrated with the transcriptome data obtained from 'W10' under the 0.25 and 25 μmol L^{-1} B levels (Hua *et al.* 2017), as well as 'QY10' and 'W10' under a 0.25 μmol L^{-1} B level (Hua *et al.* 2016b). Specifically, only those DEGs within the confidence intervals were retained for further functional annotation based on their putative *Arabidopsis* orthologues from the TAIR 10 database (https://www.arabidopsis.org/) and the Brassicaceae database (BRAD) (http://brassicadb.org/brad/index.php) (Cheng *et al.* 2011). The most probable candidate genes were chosen from among the DEGs based on functional annotations related to plant responses to B deficiency stress.

2.7. Validation of DGEs through quantitative real-time PCR (qRT-PCR)

qRT-PCR assays were used to verify the DGE results. The B-efficient variety 'QY10' and the B-inefficient variety 'W10' were selected for gene expression validation of the DGE. The total RNA was extracted from shoot and root tissues using TRIpure reagent following the prescribed protocol (Aidlab Biotechnologies Kit, Aidlab, China). The cDNA was synthesized using 1 μg of total RNA with the True Script RT Kit (Aidlab Biotechnologies). A CFX96TM Real-time PCR Detection System (Bio-Rad, Hercules, USA) was used to detect relative gene expression using 2× Universal SYBR Green Fast qPCR Mix (ABclonal, China) and a 40-cycle program of 95°C for 3 s, 60°C for 20 s, and 72°C for 20 s. The relative expression of each target gene was determined using the $2^{-\Delta\Delta C_T}$ approach (Livak and Schmittgen 2001). Rapeseed *EF1α* (*BnaC05g05630D*) and *Tubulin* (*BnaCnng62490D*) were used as internal reference genes. The specific primer sequences in this study are shown in Appendix C.

2.8. Candidate gene association study and haplotype analysis

The genotypes of candidate genes in the association population were obtained using vcftools software (https://vcftools.github.io/index.html). Candidate gene association analysis was performed using SNP markers in the interval from 2 kb upstream to 2 kb downstream of each candidate gene for the B efficiency-related traits using Tassel 5.0 software (Bradbury *et al.* 2007). The haplotype blocks were analyzed using HaploView software. A haplotype was determined by homozygous markers with LD (r^2)≥0.50 between the block's first and end markers. The Student's *t*-test was employed to detect the differences in B efficiency-related traits of varieties carrying various haplotypes.

2.9. Field trial measurements

For field trials, the B efficiency-related traits of representative varieties (116, 142, 170, 226, 248, 270, 272, 362, 642, 698, 710, 728, 744, 794, 198, 254, 284, 358, 378, 396, 400, 474, 508, 514, 518, 548, 566, 574, 576, 622, 704, 714, 722, 770, 924, 1,042, and 1,048) were investigated in 2018–2018 and 2019–2020 at Guotan village (30°180 N, 115°600 E, Wuxue, Hubei Province, China). The soil agrochemistry was as described by He *et al.* (2021), and the hot-water-soluble B was 0.10 mg kg^{-1}. The B fertilizer application was 15 kg ha^{-1} borax in the normal B treatment and 0 kg ha^{-1} borax in the B deficiency treatment. Each treatment in the randomized, complete block design consisted of three replicates. Each rapeseed accession was planted in three duplicate blocks, with each block containing 16 plants arranged in two rows of eight plants per replicate. Before harvesting, the plant height and number of first branches were recorded. After harvesting, all seeds were naturally dried to determine the thousand-seed weight and seed yield. The BEC was then determined by calculating the ratio of yield under the B deficiency treatment to yield under the normal B treatment. The data were analyzed using the Student's *t*-test, with significance determined at $P<0.05$ or $P<0.01$.

3. Results

3.1. Phenotypic variation in B efficiency-related traits under different B treatments

In this study, the four B efficiency-related traits of RRL, SDW, RDW, and BEC, were measured in a 391 rapeseed natural population under NB and LB conditions in a hydroponic system. The phenotypic variations in seedling growth responses to B deficiency were recorded. The frequency distributions of all the investigated traits under different B treatments were continuous distributions, and each one was close to a normal distribution (Fig. 1-A; Appendix D). The Kolmogorov-Smirnov normality test indicated that SDW-NB and RDW-NB did not fit a normal distribution ($P<0.001$), while the other traits were normally distributed ($P>0.05$) (Table 1). All traits showed extensive phenotypic variations among the 391 lines (Table 1; Appendices E and F). The mean values of all measured traits were considerably lower under the LB treatment compared to the NB treatment. In addition, the coefficients of variance (CV%) showed similar variability across the NB and LB treatments for RRL, SDW, and RDW (Table 1; Appendices E and F). All traits showed wide genetic variations for the association analyses. The plant growth traits of SDW, RDW, and RRL exhibited higher H^2 under the LB condition than under the NB condition, indicating the LB treatment had a more stable genetic influence and less environmental impact on plant growth (Table 1). In addition, a correlation analysis was conducted to assess the associations that exist between the phenotypes in the 391 rapeseed lines. Positive correlations were found between RRL, SDW, and RDW under both NB and LB conditions, with SDW and RDW showing particularly high correlations of r=0.81 and 0.84, respectively. Furthermore, BEC was correlated positively with the other traits exclusively in the LB condition (Fig. 1-B; Appendix D), indicating that B efficiency is not independently regulated.

3.2. Population structure and relative kinship of the association panel

The study of population structure and relative kinship was conducted using 1,507,767 SNPs with missing data less than 0.2 and MAF greater than 0.05 from the whole *B. napus*

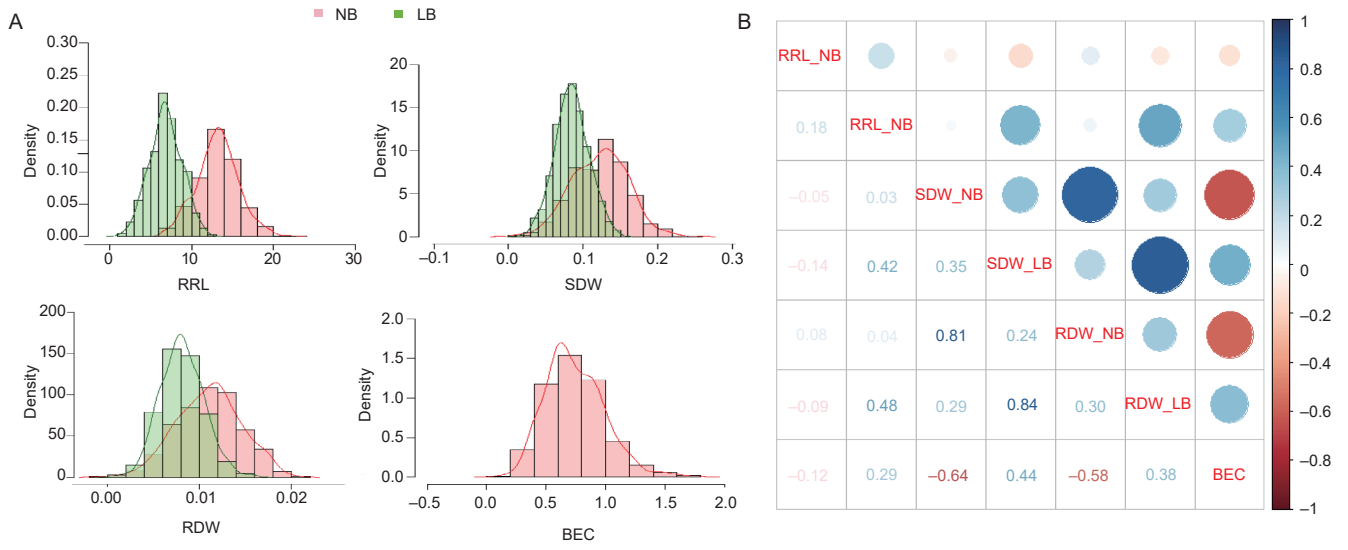


Fig. 1 Frequency distribution and correlation analysis of boron (B) efficiency-related traits of the natural rapeseed population under different B treatments. A, frequency distribution histograms; pink represents normal B level (NB), and green represents low B level (LB). B, statistical results of the correlation analysis; the numbers represent correlation coefficients, and the circle size and color intensity are proportional to the correlation coefficients. Blue indicates a positive correlation, and red indicates a negative correlation. RRL, relative root length; SDW, shoot dry weight; RDW, root dry weight; BEC, boron efficiency coefficient.

Table 1 Statistical analysis of boron (B) efficiency-related traits under different B treatments in rapeseed

Trait[1)]	Treatment[2)]	Mean±SD (*n*=391)	Min	Max	CV (%)	*P*	Heritability (H^2) (%)
RRL (cm)	NB	13.41±2.91	3.4	35.9	21.7	0.6880	78.7
	LB	6.78±2.55	0.4	14.99	36.4	0.7352	98.7
SDW (g)	NB	0.1238±0.0416	0.0325	0.2995	33.6	0.0003***	71.0
	LB	0.0838±0.0304	0.0160	0.1879	37.9	0.2815	99.8
RDW (g)	NB	0.0111±0.0048	0.0034	0.0648	43.2	0.0006***	88.5
	LB	0.0082±0.0041	0.0036	0.0448	48.5	0.0558	99.8
BEC	LB/NB	0.75±0.33	0.11	1.21	45.6	0.1540	99.8

[1)] RRL, relative root length; SDW, shoot dry weight; RDW, root dry weight; BEC, boron efficiency coefficient.
[2)] NB, normal B level; LB, low B level.
***, significant at $P<0.001$ for the Kolmogorov-Smirnov test.

genome. The ΔK value showed its sharpest peak when K=4 (Fig. 2-A), dividing the accessions into four sub-populations (Fig. 2-C). Genetic relatedness analysis revealed that the genetic relatedness among most of the accessions is below 0.1 (Fig. 2-B; Appendices G and H), indicating that the associations are distantly related to one another and thus suitable for association analysis. The LD decay refers to the distance on the chromosome where the average pairwise correlation coefficient (r^2) between all pairs of SNP markers declines to half of its greatest value. The genome-wide LD decay was analyzed for all 391 rapeseed accessions, with an average distance of 300 kb when r^2 dropped to 0.1 (Fig. 2-D).

3.3. Genome wide association analysis for B efficiency-related traits

The two models of GLM and MLM were used to conduct association analyses with the four B efficiency-related traits to assess the effects of Q and K. The Q+K model is able to effectively control false positive associations and prevent false negative associations (Cai *et al.* 2014). The GLM analysis identified a total of 765 SNPs, whereas the MLM analysis identified 106 SNPs (Table 2; Appendix I). The GWAS results for these traits, including Manhattan and Q-Q plots, are presented in Appendices I and J. As expected, these significant association loci contain many known B-related genes (Appendices K–M), proving the potential of GWAS to find candidate genes. The significantly associated SNPs are unevenly distributed across all chromosomes. Specifically, the SNPs significantly associated with all four traits under the low B condition are mostly concentrated on chromosomes A03 and C03 (Fig. 3). Among them, two significant SNPs, Bna-A03-p14387835 and Bna-A03-p14464672, were found to be associated with SDW and RDW based on GLM and MLM. In addition, the significant SNP of Bna-C03-p20410319 was associated with SDW and RDW based on GLM and MLM. Bna-C03-p21835492 was associated with RDW and BEC based on both GLM and MLM (Appendix L). Potential candidate genes for significant marker-trait associations were identified by detecting all genes located within a 300 kb physical distance on both sides of each SNP. Among the results, a significant SNP cluster associated with SDW, RDW and RRL was co-localized on the chrA03: 14,087,835–14,764,672 interval at the LB level, which overlapped with the previously reported QTL *qBEC-A3a*

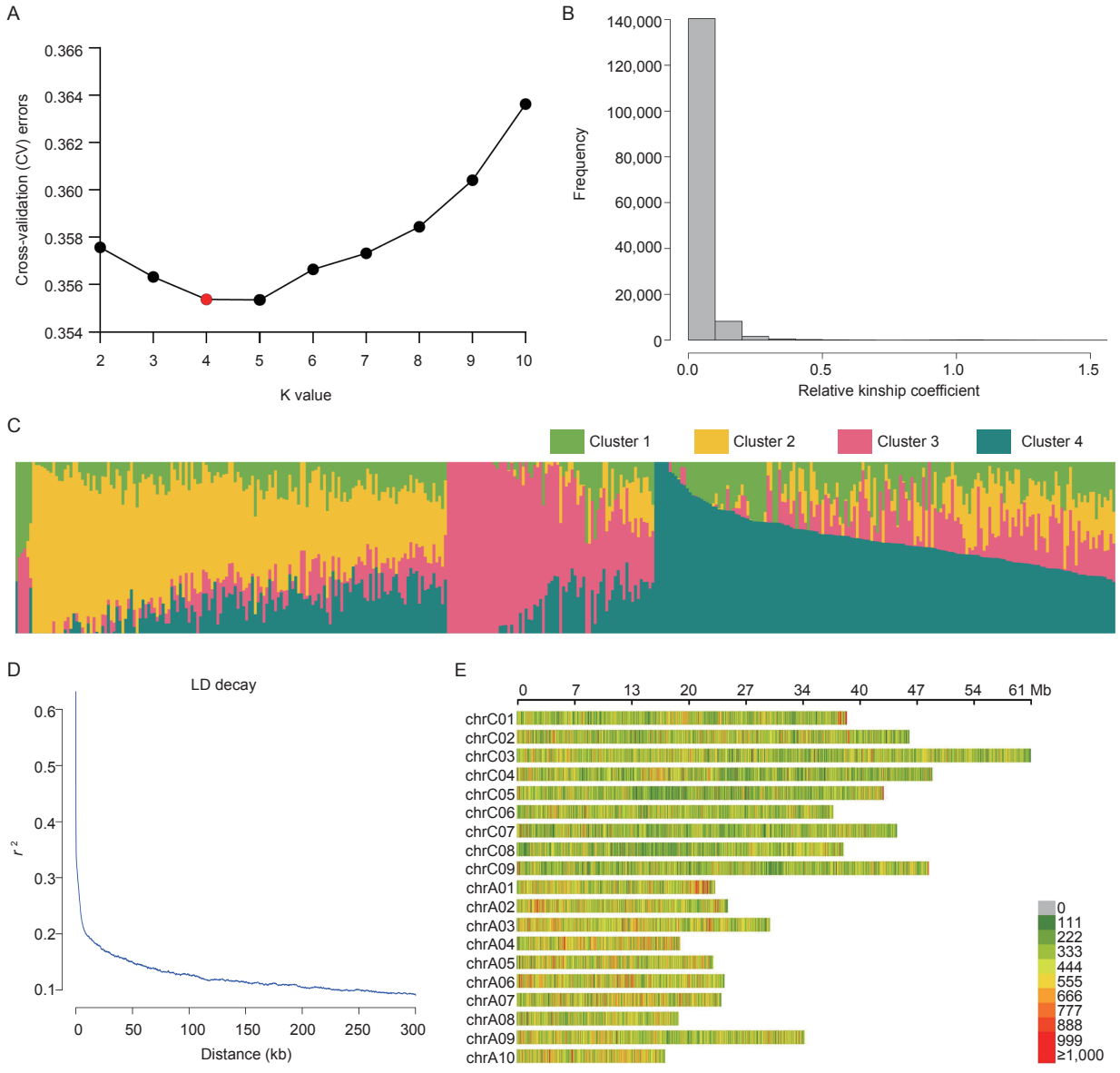


Fig. 2 Analysis of the genetic polymorphisms of 391 rapeseed accessions. A, kinship (K) values were estimated for population structure analysis. There was a minimum K value when K=4. B, distribution of pairwise relative kinship coefficients of 391 rapeseed accessions. C, population structure based on K=4. Each individual accession is represented by a vertical bar partitioned into colored segments, with the length of each segment representing the proportion of the individual's genome. D, genome-wide decay of linkage disequilibrium (LD) estimated from 391 rapeseed accessions. E, single nucleotide polymorphism (SNP) density within a 100 kb window size on the 19 chromosomes of 391 re-sequenced genomes. Different colors show the various densities as displayed in the spectrum column.

(Fig. 4-A; Appendix N; Zhang *et al.* 2014a). Another significant SNP cluster associated with SDW, RDW, RRL, and BEC was co-localized on the chrC03: 20,110,319–22,135,492 interval at the LB level (Fig. 4-B). Totals of 124 and 329 neighboring genes were significantly correlated with these significant SNPs in the cluster intervals on chromosomes A03 and C03, respectively (Appendix O).

3.4. Transcriptome analysis for identifying DEGs

To select the DEGs, the differential gene expression profiling of 'W10' in response to varying B availabilities (B sufficiency and B deficiency) was analyzed. In addition, DGE profiling was also analyzed to identify transcriptional differences between variety 'QY10', which is B-efficient, and variety 'W10', which is B-inefficient, under B deficiency. The leaves and roots showed 1,073 and 375 up-regulated genes and 1,877 and 473 down-regulated genes, respectively, under B deficiency compared to B sufficiency (Fig. 5-A). Moreover, 6,018 and 3,682 up-regulated DEGs and 4,522 and 4,776 down-regulated DEGs between 'QY10' and 'W10' were identified in the shoots and roots, respectively (Fig. 5-B). Next, the GWAS results and two transcriptome analyses were integrated to narrow down the potential candidate genes. A crossover analysis was conducted between the 453 genes on chromosomes A03 and C03 identified by GWAS and the DEGs discovered by RNA-seq. Finally, 68 candidate genes

Table 2 Numbers of SNPs and phenotypic explained rates of boron (B) efficiency-related traits identified based on the general linear model (GLM) and mixed linear model (MLM) under different B treatments

Trait[1)]	Model	Number of SNP (normal B, NB)	Number of SNP (low B, LB)	Phenotypic explained variation (PEV_NB) (%)	Phenotypic explained variation (PEV_LB) (%)
RRL	GLM	124	48	5.84–10.52	6.33–11.05
	MLM	11	1	7.20–9.60	7.35
SDW	GLM	67	125	6.37–11.75	5.67–10.81
	MLM	9	18	7.29–10.96	6.78–10.82
RDW	GLM	39	311	6.70–11.83	5.84–11.24
	MLM	9	53	7.30–12.15	6.81–11.72
BEC	GLM	51		6.19–9.94	
	MLM	5		7.89–9.93	

[1)] RRL, relative root length; SDW, shoot dry weight; RDW, root dry weight; BEC, boron efficiency coefficient.

in shoots and 48 candidate genes in roots were co-selected from the GWAS and transcriptome DEGs, among which five and four candidate genes overlapped in the GWAS and the two transcriptome analyses in shoots and roots, respectively (Fig. 5-C). Overlapped gene IDs and their annotations were listed in Appendix P.

3.5. qRT-PCR validation of DEGs and exploration of candidate genes related to B efficiency

To further identify the candidate genes controlling B efficiency-related traits in *B. napus*, the expression patterns of the overlapping genes, 68 candidate genes in shoots and 48 candidate genes in roots, were determined by analyzing the transcription results (Fig. 6-A and B). Given the higher differentially expressed fold-change and major biological functions involved in plant growth and nutrient uptake or transport, eight candidate genes were finally selected: *BnaA03g29020D*, *BnaA03g29440D*, *BnaA03g29990D*, *BnaA03g30330D*, *BnaC03g33010D*, *BnaC03g33890D*, *BnaC03g34490D*, and *BnaC03g35660D* (Table 3). Among them, *BnaA03g29020D*, *BnaA03g29990D*, *BnaA03g30330D*, and *BnaC03g35660D* were suggested by the crossover analysis of GWAS and both of the transcriptomes (Appendix P). To confirm the accuracy of the RNA-seq results, qRT-PCR validation was conducted to assess the expression levels of the eight candidate genes. Generally, the gene expression results showed consistency between the RNA-seq and qRT-PCR results (Fig. 6-C). According to the functional annotations of these eight candidates, four genes are engaged in transporter activity (*BnaA03g29440D*, *BnaA03g30330D*, *BnaC03g34490D*, and *BnaC03g35660D*), three in response to stimulus (*BnaA03g29020D*, *BnaA03g29990D*, and *BnaC03g33890D*), and one in transcription factor activity (*BnaC03g33010D*) (Table 3). Interestingly, these selected candidates include a B efflux transporter gene, *BnaA3.BOR3* (*BnaA03g29440D*). The qRT-PCR analysis results showed that the expression of *BnaA3.BOR3* was up-regulated in shoots and roots by B deficiency (0.1 μmol L^{-1} B) in both the B-efficient 'QY10' and B-inefficient 'W10' varieties. However, under the normal B condition (30 μmol L^{-1} B), the *BnaA3.BOR3* expression in B-inefficient 'W10' was significantly higher than that in B-efficient 'QY10' in both shoots and roots. Conversely, the increase in expression induced by B deficiency in B-efficient 'QY10' was considerably greater than that in B-inefficient 'W10', indicating a significant role of this gene in efficient B transport (Fig. 6-C).

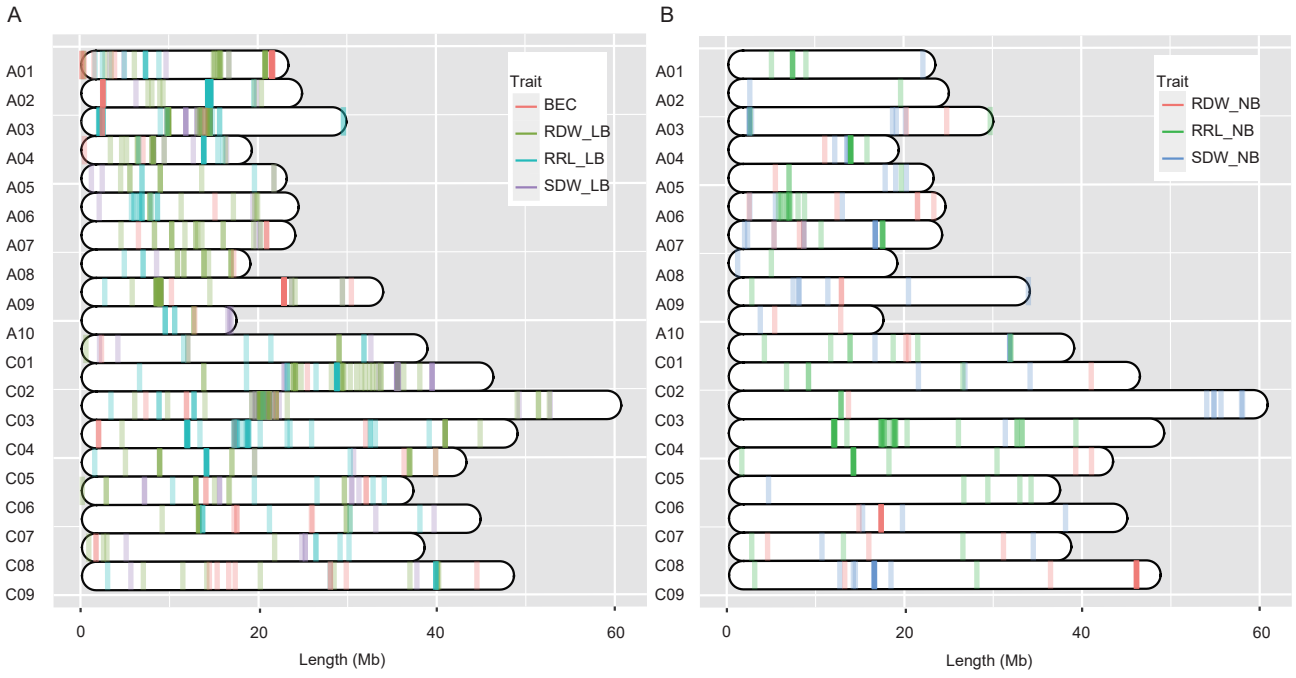


Fig. 3 Distribution on the rapeseed reference genome of single nucleotide polymorphisms (SNPs) significantly associated with boron (B) efficiency-related traits under different B treatments. BEC, boron efficiency coefficient; RDW, root dry weight; RRL, relative root length; SDW, shoot dry weight. LB, low B level; NB, normal B level.

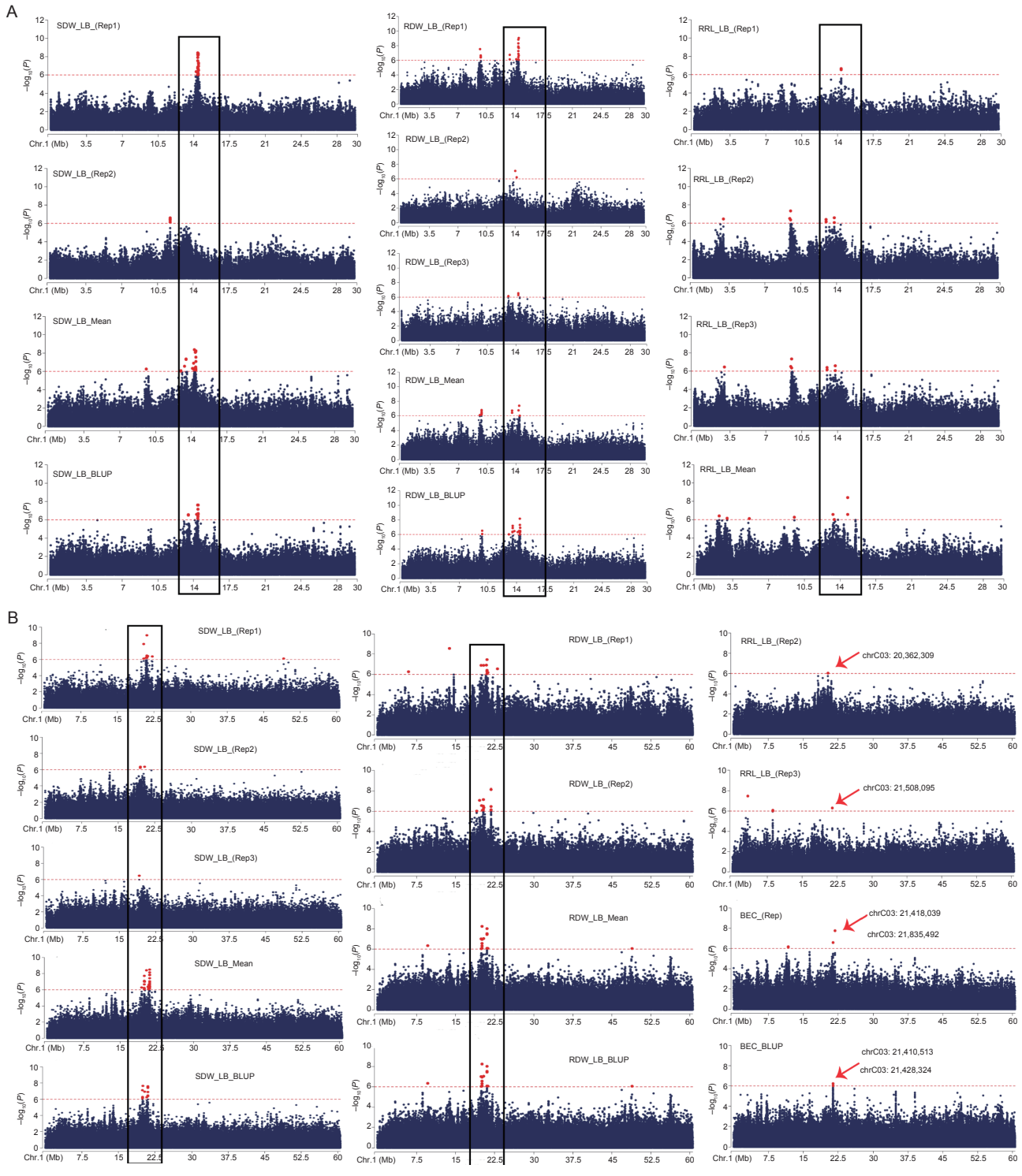


Fig. 4 Co-localized clusters on chromosomes A03 and C03 associated with boron (B) efficiency-related traits in an association panel of 391 rapeseed accessions. A, Manhattan plots of the co-localized cluster (chrA03: 14,087,835–14,764,672) for shoot dry weight (SDW), root dry weight (RDW), and relative root length (RRL) at the low B (LB) level on chromosome A03. B, Manhattan plots of the co-localized cluster (chrC03: 20,110,319–22,135,492) for SDW, RDW, RRL, and boron efficiency coefficient (BEC) at the LB level on chromosome C03. The large red dots represent the significant SNPs, the black boxes indicate co-localized SNP clusters, and the red arrows indicate co-localized single nucleotide polymorphisms (SNPs). BLUP, the best linear unbiased prediction.

3.6. Identification of candidate genes by candidate gene association analysis

Next, the SNPs of the eight candidate genes were compared (Fig. 6; Table 3). The SNPs on *BnaA03g29990D*, *BnaA03g30330D*, *BnaC03g33890D*, and *BnaC03g35660D* may not be responsible for the B efficiency-related traits, either because there were no significant SNPs within the promoter and coding regions of the candidate genes, or

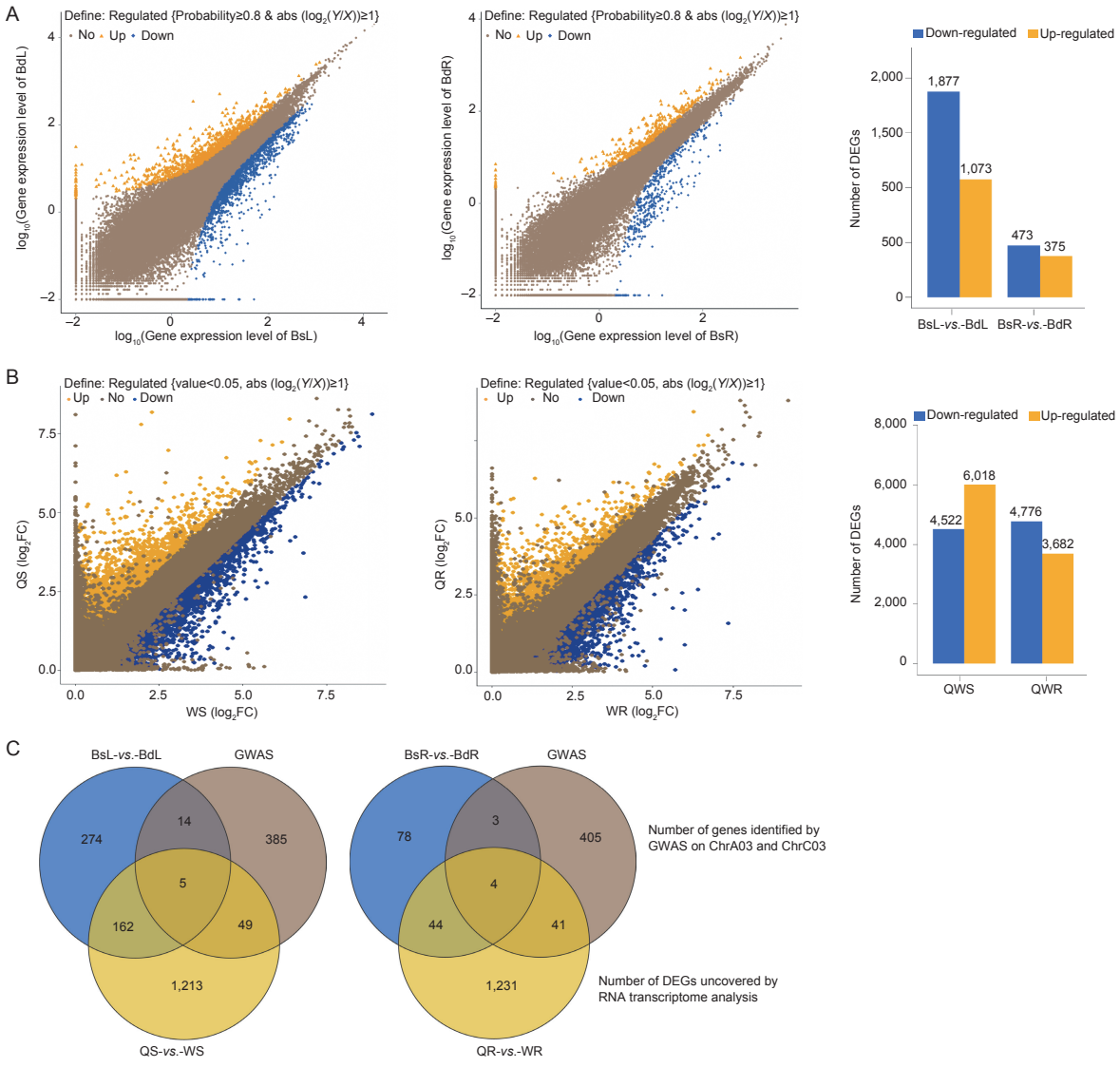


Fig. 5 Differentially expressed genes (DEGs) revealed by transcriptome analysis. A, scatter plots and counts of the DEGs detected in the leaves (L) and roots (R) of rapeseed seedlings, which were cultivated under boron (B) deficiency (0.25 μmol L^{-1} B, Bd) and B sufficiency (25 μmol L^{-1} B, Bs) for 10 d. B, scatter plots and counts of the DEGs detected in the shoots (S) and R of 'QY10' (Q) and 'W10' (W) seedlings, which were cultivated under B deficiency (0.25 μmol L^{-1} B) for 10 d. C, Venn diagram showing the number of candidate genes identified by genome-wide association study (GWAS) on ChrA03 and ChrC03, the number of DEGs revealed by RNA-seq analysis, and the number of overlaps.

the significant SNPs in the coding region are synonymous mutations that do not alter the amino acid sequence. Therefore, these four genes were excluded from the subsequent analysis. A total of 22 SNPs were found to be linked with *BnaA03g29440D*, only two of which resulted in amino acid changes. Notably, the SNP chrA03_14318092 exhibited significant associations with SDW, RDW, and RRL (Fig. 7-A and B), and resulted in a substitution of the encoded amino acid from cysteine (Cys) to glycine (Gly). In addition, another significant SNP, chrA03_14318601, displayed significant association with SDW and RDW (Fig. 7-A and B) and led to a change in an encoded amino acid from valine (Val) to isoleucine (Ile). Haplotype analysis detected two major haplotypes: AC and CT (Appendix Q). Next, comparative phenotype analyses showed that the accessions with haplotype allele Hap2_CT had higher B efficiency-related trait values compared with the Hap1_AC under low B conditions (Fig. 7-C), indicating that Hap2 (CT) is a favorable haplotype and that the genetic variation of *BnaA03g29440D* is significantly associated with B efficiency.

There were 23 significant SNPs tightly linked with *BnaA03g29020D*, of which those located in the CDS region are all synonymous mutations, preserving the amino acid sequences unaltered. Thus, we focused on the SNPs located in the promoter region, among which chrA03_14118351 and chrA03_14119764 exhibited significant associations with SDW, RDW, and RRL under low B conditions (Appendix R). Haplotype analysis detected two major haplotypes: CT and AC (Appendix Q). Comparative phenotype analyses showed that the accessions with haplotype allele Hap2_AC had higher SDW, RDW, and RRL values compared with Hap1_CT (Appendix R), indicating

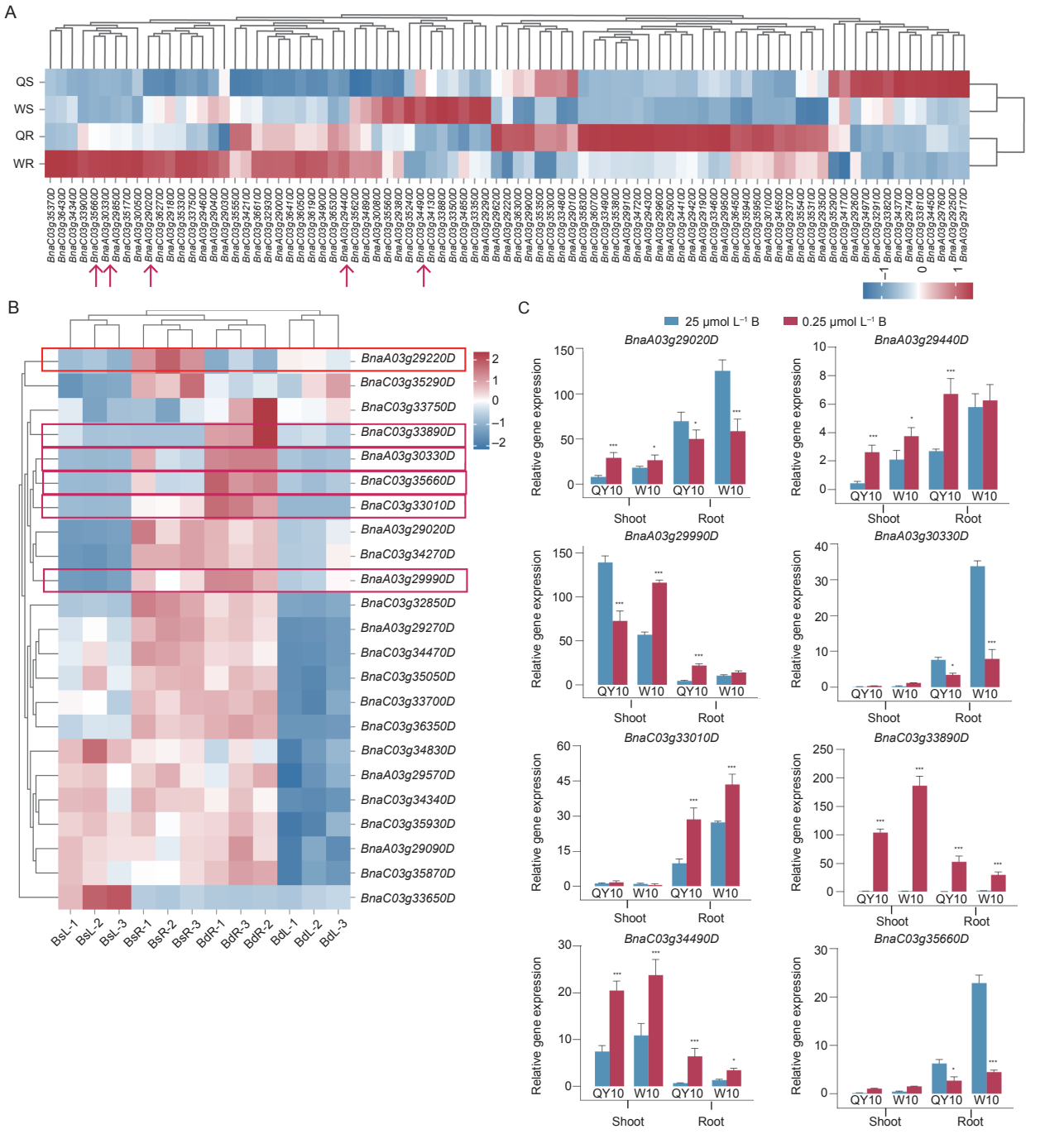


Fig. 6 Differences in the expression of candidate genes narrowed down by genome-wide association study (GWAS) and transcriptome analysis. A, heatmap of the expression patterns of candidate genes overlapping between genes identified in GWAS and differentially expressed genes (DEGs) in the shoots (S) and roots (R) of 'QY10' (Q) and 'W10' (W) seedlings under boron (B) deficiency (0.25 μmol L^{-1} B, Bd). B, heatmap of the expression patterns of candidate genes overlapping between genes identified in GWAS and DEGs in the leaves (L) and roots (R) of rapeseed seedlings under Bd and B sufficiency (25 μmol L^{-1} B, Bs) conditions. C, validation of candidate gene expression levels by RT-qPCR in the shoots and roots of 'QY10' and 'W10' seedlings, which were cultivated under Bd and Bs conditions for 10 d. Red arrows and red boxes indicate differentially expressed candidate genes identified by GWAS and transcriptome analysis, respectively. Data are shown as mean±SD, n=4 biological replicates, with 15 plants per replicate. *, P<0.05; ***, P<0.001; two-tailed unpaired Student's t-test.

that Hap2 (AC) is a favorable haplotype associated with B efficiency. In addition, 73 significant SNPs were tightly linked with *BnaC03g33010D*. Among them, only one SNP, chrC03_20207218, was located in a CDS that is significantly associated with SDW and RDW and a non-synonymous mutation, leading to a change in the encoded amino acid from serine (Ser) to asparagine (Asn) (Appendices Q and R). Comparative phenotype analyses showed that accessions with chrC03_20207218_C showed significantly higher SDW and RDW values than those with chrC03_20207218_T under B deficiency conditions (Appendix R), indicating that Asn is favorable, and the genetic variation of *BnaC03g33010D* is

Table 3 Candidate genes narrowed down by genome-wide association study (GWAS) and transcriptome analysis and their annotations

Number	Gene ID	Homologous gene	Pfam_annotation	Nr_annotation
1	*BnaA03g29020D*	*AT3G05490*	Rapid ALkalinization Factor (RALF)	Ralf-like 22 (RLF22)
2	*BnaA03g29440D*	*AT3G06450*	HCO_3^- transporter family	Boron transporter
3	*BnaA03g29990D*	*AT3G07390*	Protein of unknown function (DUF568)	Auxin-induced in root cultures 12 (AIR12)
4	*BnaA03g30330D*	*AT3G08040*	MatE	Ferric reductase defective 3 (FRD3)
5	*BnaC03g33010D*	*AT3G02550*	Lateral organ boundaries (LOB) domain	LOB domain-containing protein 41 (LBD41)
6	*BnaC03g33890D*	*AT3G04720*	Barwin family	Pathogenesis-related 4 (PR4)
7	*BnaC03g34490D*	*AT3G05960.1*	Sugar (and other) transporter	Sugar transport protein 6 (STP6)
8	*BnaC03g35660D*	*AT3G08040*	MatE	Ferric reductase defective 3 (FRD3)

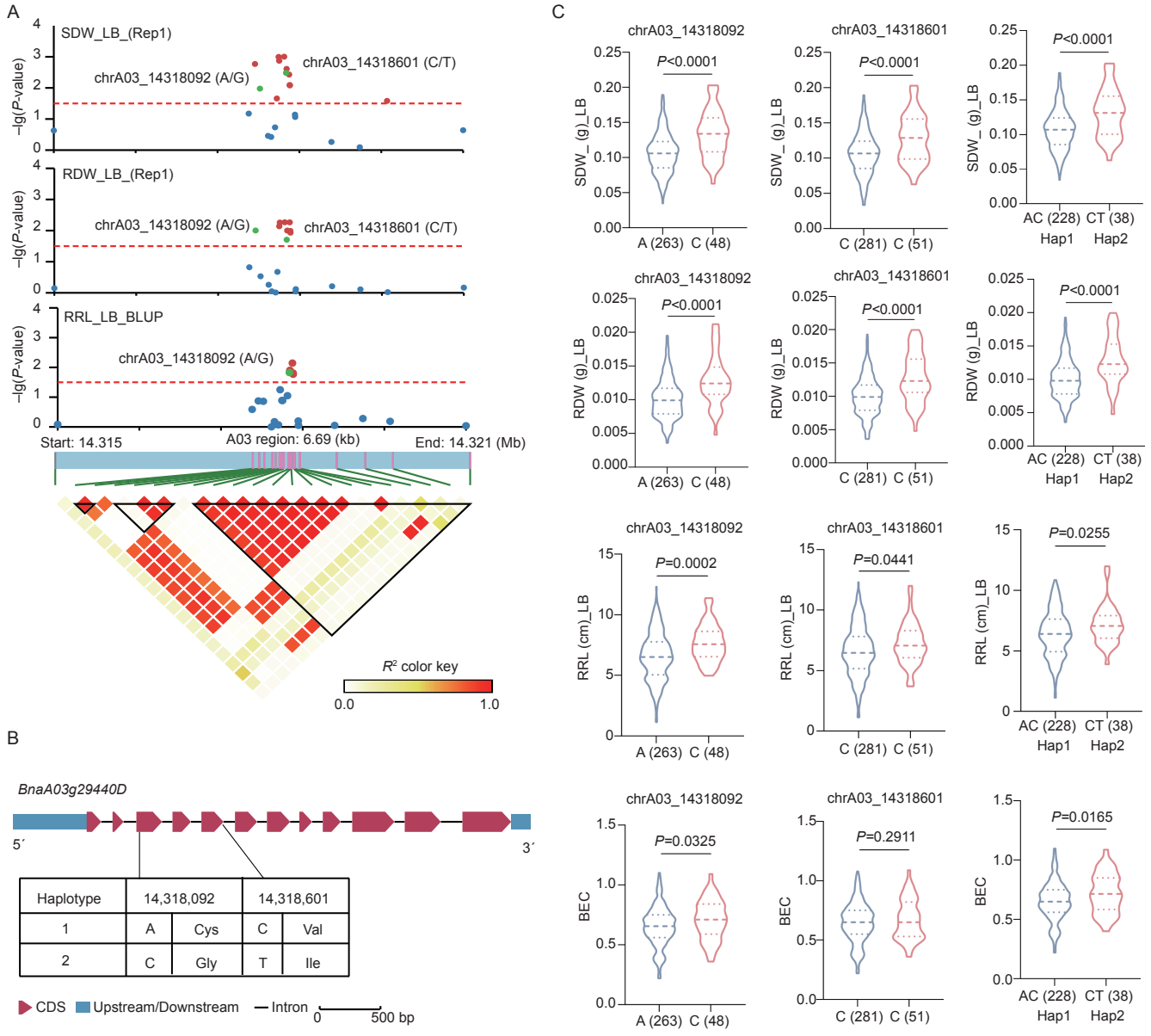


Fig. 7 Natural variations in *BnaA03g29440D* significantly associated with boron (B) efficiency-related traits in rapeseed. A, association analysis of genetic variation in *BnaA03g29440D* with shoot dry weight (SDW), root dry weight (RDW), and relative root length (RRL) in rapeseed. The large red dots represent significant single nucleotide polymorphisms (SNPs). The green dots represent significant SNPs co-localized with multiple traits. LB, low B level. B, schematic diagram of the 3,884 bp genomic fragment, including 551 bp 5′-UTR, 147 bp 3′-UTR, the protein coding region, and the location of two significantly associated SNPs that formed two haplotypes of *BnaA03g29440D*. C, comparison of four B efficiency-related traits for Hap1 and Hap2 in 391 rapeseed lines. Hap1 and Hap2 represent B inefficient and efficient alleles, respectively. The numbers in brackets represent the genotype numbers of the two alleles. Statistical significance was determined by Student's *t*-test. Hap, haplotype.

significantly associated with B efficiency. Furthermore, 86 significant SNPs were tightly linked with *BnaC03g34490D*, among which the SNPs located in CDS that are significantly associated with B efficiency-related traits were all synonymous mutations. Further, the SNPs located in promoter regions, chrC03_20203734 and chrC03_20203751, exhibited significant associations with B efficiency-related traits under the LB condition (Appendix R). Haplotype analysis identified three major haplotypes: AT, AC, and GC (Appendices Q and R). Comparative phenotype analyses showed that accessions with haplotype allele Hap3_GC had the highest SDW, RDW, RRL, and BEC values compared to either Hap1_AT or Hap2_AC, while there were no significant differences between Hap1_AT and Hap2_AC (Appendix R), indicating that Hap3 (GC) is a favorable haplotype and that the genetic variation of *BnaC03g34490D* is significantly associated with B efficiency.

3.7. Favorable haplotypes confer high B efficiency to the natural population

From the natural population, 14 B-efficient and 23 B-inefficient rapeseed accessions were chosen to examine the associations between favorable haplotypes and B efficiency (Appendix S). All 14 B-efficient accessions (BEA) contained favorable haplotypes of *BnaA03g29020D*, *BnaA03g29440D*, and *BnaC03g34490D*, whereas all 23 B-inefficient accessions (BIA) contained non-favorable haplotypes of *BnaA03g29020D*, *BnaA03g29440D*, *BnaC03g33010D*, and *BnaC03g34490D*. These accessions were used to evaluate B efficiency in seedling traits and field trials with NB and LB treatments. Under NB conditions, there were no obvious differences between the BEA and BIA at the seedling stage (Fig. 8-A and B; Appendices S and T). Under LB conditions, BIAs such as 474, 514, and 704 showed severe root growth inhibition and biomass reduction compared with the BEAs such as 270, 362, and 710 at the seedling growth stage (Fig. 8-A). Consistent with these results, the RRL, SDW, RDW, and BEC of BEAs with favorable haplotypes were significantly higher than those of BIAs with non-favorable haplotypes under the LB condition (Fig. 8-B; Appendix S). Subsequent field studies examined whether the B-efficient and -inefficient haplotypes differed in seed yield and yield-related traits under different B treatments. The plant heights, numbers of first branches, thousand-seed weights, seed yields, and boron efficiency coefficients of BEAs carrying favorable haplotypes were better than those of the BIAs presenting the non-favorable haplotypes (Fig. 8-C and D; Appendix S). Overall, the genetic variations of these candidate genes in various rapeseed cultivars further confirmed that the favorable haplotypes enhanced plant growth and production under B deficiency conditions, ultimately conferring high B efficiency to the natural population.

4. Discussion

4.1. Variation in phenotypes across various B levels

Due to large genotypic variability, rapeseed cultivars respond differently to B deficiency conditions, which severely inhibits their growth and development (Hua *et al.* 2016b). To mine the genes controlling B uptake, transport, and utilization and find excellent haplotypes associated with B efficiency, a genome-wide association study (GWAS) was used to explore the excellent alleles that control B efficiency-related traits. As a powerful method for candidate gene discovery, GWAS has effectively revealed the genetic basis of several agriculturally significant traits in various crops (Xiao *et al.* 2017). This study is the first attempt, as far as we know, to conduct a GWAS for the B efficiency-related traits of the rapeseed natural population under NB and LB conditions at the seeding stage. The availability of appropriate genotypes is critical for identifying significant SNPs and haplotypes. Indeed, B deficiency symptoms initially manifest in the younger leaves and the newly formed apex, such as root tips, drastically reducing the root length and biomass (Brown *et al.* 2002). Thus, this study investigated genotypic parameters directly associated with B efficiency in rapeseed, including RRL, SDW, RDW, and BEC (Table 1; Fig. 1). Moreover, the genetic basis for variation in these four B efficiency-related traits was investigated across a natural population comprising 391 rapeseed accessions. In comparison to the normal B condition, B deficiency resulted in higher coefficients of variation (CV%) and H^2, indicating that some excellent alleles participate in regulating the B deficiency-induced phenotypic variance (Table 1; Appendices E and F). A genetic inheritance study of B efficiency in rapeseed revealed that it is a quantitative trait (Xu *et al.* 2002). Similarly, this study also observed that the four trait phenotypes were all fitted to either a normal distribution or approximately normal distribution (Table 1; Fig. 1-A; Appendix D). In addition, the correlations between SDW and RDW were significantly higher than those observed with the other traits (Table 1; Fig. 1-B; Appendix D), implying that there are common genes involved in the responses of SDW and RDW to low B stress.

4.2. GWAS for B efficiency-related traits and candidate genes for B efficiency in rapeseed under LB conditions

The SNPs for multiple traits overlapped due to the significant positive correlations between the tested traits across B levels (Fig. 1-B; Appendix D). The correlation and co-localization of SNPs among the examined traits revealed a similar molecular regulation of the physiological processes. In this study, the SNPs for four traits were found to overlap with each other on chromosomes A3 and C3 under the LB condition, whereas such overlap was not observed under the NB condition (Figs. 3 and 4). Thus, we primarily focused on two SNP clusters on chromosomes A03 and C03, chrA03: 14,087,835–14,764,672 and chrC03: 20,110,319–22,135,492, that were detected across multiple traits (Figs. 3 and 4). Early studies identified numerous QTLs for B efficiency traits in rapeseed across various populations. For example, QTLs associated with B efficiency in rapeseed were detected using F_2 or DH populations obtained from a breeding hybrid between QY10 and Bakow (Xu *et al.* 2001; Zhao *et al.* 2008, 2012) and a DH population from a cross between QY10 and W10 (Zhang *et al.* 2014a). Here, we

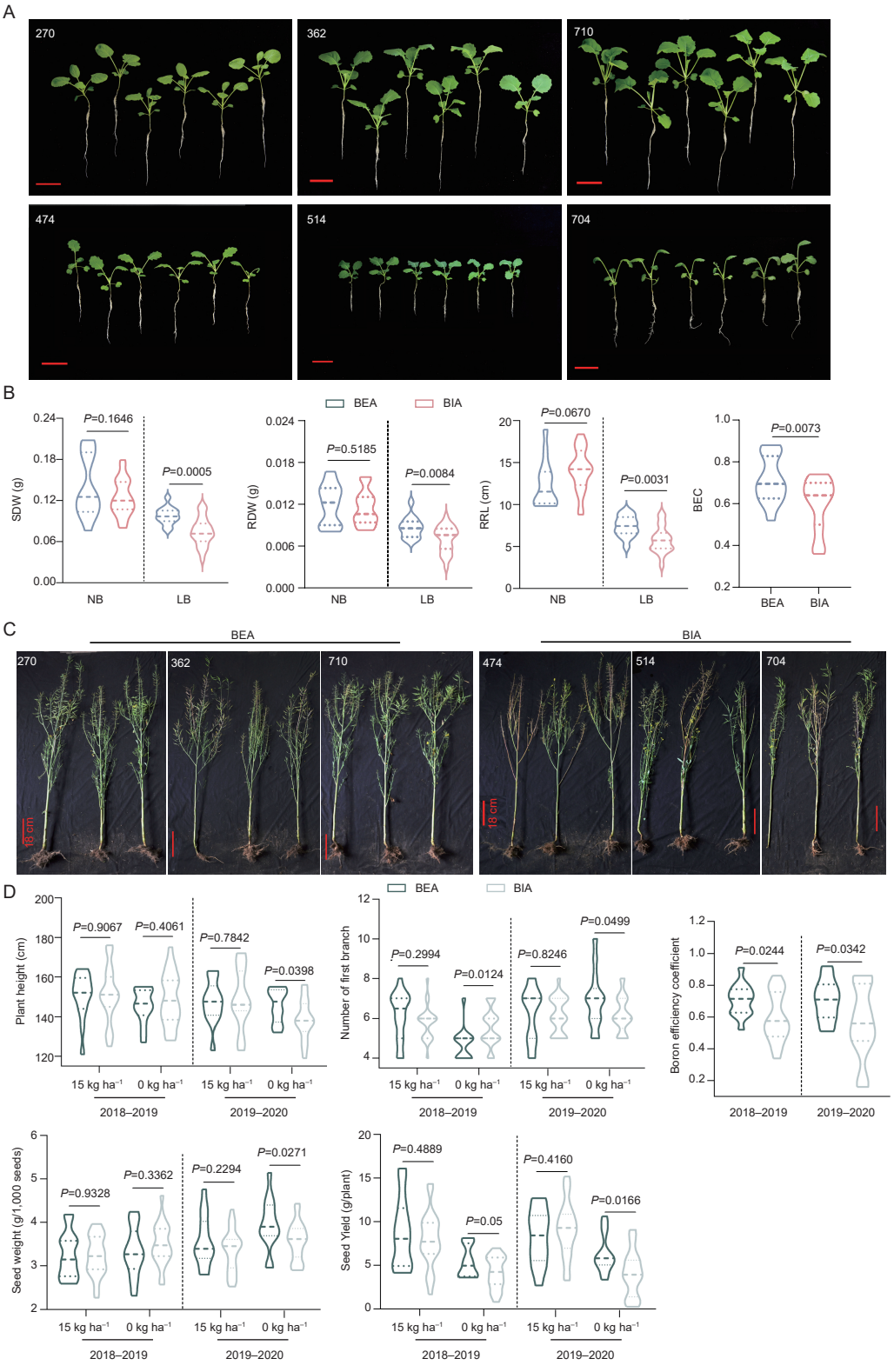


Fig. 8 Validation of boron (B) efficiency-related traits between accessions with B-efficient and -inefficient haplotypes at the seedling and mature stages. A, phenotypic differences of B-efficient and -inefficient variety seedlings cultured under low B treatment (0.25 μmol L^{-1} B, LB) for 15 d. The numbers 270, 362, and 710 are accessions with B-efficient haplotypes, while 474, 514, and 704 are accessions with B-inefficient haplotypes. Scale bars=5 cm. B, differences in the B efficiency-related traits between rapeseed accessions with B-efficient and -inefficient haplotypes at the seedling stage. SDW, shoot dry weight; RDW, root dry weight; RRL, relative root length; BEC, B efficiency coefficient. NB, normal B level. BEA, boron efficient accessions; BIA, boron inefficient accessions. C, phenotypic differences of B-efficient and -inefficient varieties of plants at the mature stage under a deficient B supply (0 kg ha^{-1}). Scale bars=18 cm. D, differences in the seed yield and yield-related traits of plant height (cm), number of first branches, seed weight (g/1,000 seeds), seed yield (g/plant), and BEC between rapeseed accessions with B-efficient and -inefficient haplotypes at a normal B supply (15 kg ha^{-1}) and a deficient B supply in 2018–2019 and 2019–2020. Statistical significance was determined by Student's *t*-test.

compared the physical positions of significant SNPs found in our analysis with QTLs from prior studies using the Darmor-*bzh* genome as a reference. Nine significant SNPs detected by GWAS in the interval of chrA03: 14,087,835–14,764,672 were found to co-localize with the intervals of the stable major QTL *qBEC-A3a* (Appendix N). As far as we know, *qBEC-A3a* is a major QTL for B efficiency (Zhang *et al.* 2014a). In addition, Hua *et al.* (2016a) found a NODULIN 26-LIKE INTRINSIC PROTEIN (*NIP*) gene underlying the major B uptake efficiency QTL *qBECA3a* in rapeseed by combining QTL fine mapping. This finding suggests that candidate genes within the SNP cluster interval on chromosome A03 are likely to be linked to B efficiency in the rapeseed natural population. In addition to co-located SNPs with QTLs, other novel loci were detected in the SNP cluster intervals. Based on the permissive model GLM, we detected numerous significant SNPs, which might potentially introduce more false positives than the strict MLM model. Therefore, to reduce false positives, this study found that these four loci, Bna-A03-p14387835, Bna-A03-p14464672, Bna-C03-p20410319, and Bna-C03-p21835492, could be identified based on the MLM across multiple traits, implying the high reliability of these association signals in the SNP cluster intervals on chromosomes A03 and C03 (Appendix L).

In this study, many genes previously believed to be associated with B were also identified (Appendices K–M). Among them, *BnaA02g22030D* (*BnaA2.NIP5*) and *BnaA0324370D* (*BnaA3.NIP5*) were confirmed to be crucial for *B. napus* growth under low B stress (He *et al.* 2021), which further illustrates the viability of discovering candidate genes through GWAS. Fifty loci were found to be associated with two or more traits, but most loci were only found to be associated with one trait (Appendix L), suggesting that certain loci might exert pleiotropic effects on plant growth traits in response to low B stress, whereas the B efficiency-related traits are controlled by distinct genetic loci. Considering the relatively low decay of linkage disequilibrium (LD) in rapeseed, this study defined one association locus as a 300 kb region encompassing numerous genes (Fig. 2-D; Qian *et al.* 2021); thus, pinpointing the causal genes for these loci is still rather difficult. To address these problems, multiple omics techniques have been combined with GWAS to effectively determine these associations (Lu *et al.* 2017; Chen *et al.* 2022). Therefore, we integrated the GWAS results with the transcriptome data of DEGs in response to different B conditions (Hua *et al.* 2017), as well as the DEGs observed between distinct genotypes under B deficiency conditions (Zhou *et al.* 2016), and ultimately mined eight candidate genes based on gene expression patterns and biological functions (Fig. 6; Table 3).

4.3. Genetic control of B efficiency-related traits and exploration of favorable haplotypes in rapeseed

These eight candidate genes were found to be associated with ion transport and signal responses (Table 3). The influx channel proteins and efflux-type transporters for B were functionally characterized to determine plant B uptake and translocation (Takano *et al.* 2002, 2005). Of special interest, *BnaA03g29440D* (*BnaA3.BOR3*) was identified as the plausible candidate gene in this study. qRT-PCR validation showed that under the normal B condition, the *BnaA3.BOR3* expression level in the B-efficient 'W10' was significantly lower than that of the B-inefficient 'QY10', and the expression level induced by B deficiency showed a significantly greater increase in 'QY10' than in 'W10' (Fig. 6-C), indicating that *BnaA3.BOR3* might be a high-affinity B transporter for achieving efficient B transport. Another gene, *BnSUT6* (*BnaC03g34490D*), an ortholog of *AT3G05960*, encodes the sugar transport protein 6 (STP6) (Liu *et al.* 2022). AtSTP6 is a H^+-monosaccharide symporter that has significant potential to enhance plant stress tolerance (Scholz-Starke *et al.* 2003; Kong *et al.* 2019). Studies have revealed that the abundance and deficiency of B nutrients in rapeseed significantly impact photosynthesis efficiency and carbohydrate metabolism (Camacho-Cristóbal *et al.* 2008; Tan *et al.* 2016). Thus, we considered that the genetic variation of *BnSUT6* is likely to be involved in the carbohydrate metabolism process of *B. napus* in response to low B stress. Other candidate genes were associated with signal responses. *BnaA03g29020D* encodes an ortholog of rapid alkalinization factor 22 (*RALF22*, *AT3G05490*), which is required for pectic HG demethylesterification and self-assembly (Schoenaers *et al.* 2024). B-mediated RG-II cross-linking is widely recognized to play a crucial role in cell wall assembly (Chormova *et al.* 2014). Thus, RALF22 might be linked with the reduced RG-II dimerization and pectin esterification caused by B deficiency (Zhang *et al.* 2022). *BnaC03g33010D* encodes an ortholog of the lateral organ boundaries (LOB) domain-containing protein 41 (*LBD41*, *AT3G02550*). Studies have shown that LBD genes can participate in regulating the accumulation of brassinosteroids (BR) (Bell *et al.* 2012) and cooperate with auxin (Bureau *et al.* 2010), jasmonic acid (JA) (Thatcher *et al.* 2012), and cytokinin (CK) (Naito *et al.* 2007) to regulate plant growth. In addition, B nutrition in *B. napus* is closely related to hormone responses (Zhou *et al.* 2016). These results suggest that the genetic variation of *BnaC03g33010D* might be involved in the hormone-regulated process of *B. napus* in response to low B stress.

We compared the SNPs of the four candidate genes that exhibited significant associations with B efficiency-related traits. The significantly associated SNPs in *BnaA03g29020D* and *BnaC03g34490D* were in the promoter region (Appendix R), and alterations in promoter sequences are known to affect gene expression levels (Fu *et al.* 2024; Lin *et al.* 2024). There were two significantly associated SNPs in the coding region of *BnaA03g29440D*, and one SNP in the coding region of *BnaC03g33010D* (Fig. 7; Appendix R). Studies have shown that both synonymous and nonsynonymous mutations frequently disturb the level of mRNA expression of the mutated gene (Shen *et al.* 2022). Thus, these results suggest that the significant SNPs in the promoter or coding region of candidate genes might result in differential gene expression in response to various B treatments. Furthermore, these significant SNPs formed distinct haplotypes, which might also lead to differential gene expression in various varieties (Appendix Q; Fig. 6). Favorable haplotypes could increase

rapeseed B efficiency under LB conditions, thereby improving plant growth and rapeseed yield (Fig. 8; Appendices S and T).

5. Conclusion

In general, enhancing the population frequency of beneficial alleles is one of the primary goals of crop breeding. High-density, high-throughput SNP markers derived from re-sequenced populations provide valuable insights for identifying and analyzing the beneficial alleles associated with a specific target trait. For a relatively thorough analysis of the genetic architecture concerning B efficiency in *B. napus*, this study employed a GWAS with 391 accessions for B efficiency-related traits at the seedling stage under NB and LB conditions, which uncovered many unreported loci or genes associated with B efficiency-related traits. Transcriptome sequencing databases and bioinformatic analysis helped us to identify the B efficiency-related trait causative genes in significantly associated regions. The association loci and causal genes identified in this study are valuable resources for further experimental verification and will help researchers to understand the molecular mechanism of B efficiency and to genetically improve B deficiency resistance in future research.

Acknowledgements

This work was supported by the National Natural Science Foundation of China (32372805 and 31972483).

Declaration of competing interest

The authors declare that they have no conflict of interest.

Declaration of generative AI and AI-assisted technologies in the writing process

The authors declare that they did not use AI in the preparation and writing of this manuscript.

Appendices associated with this paper are available at https://doi.org/10.1016/j.jia.2024.11.013

References

Alexander D H, Novembre J, Lange K. 2009. Fast model-based estimation of ancestry in unrelated individuals. *Genome Research*, **19**, 1655–1664.

Begum R A, Fry S C. 2022. Boron bridging of rhamnogalacturonan-II in Rosa and *Arabidopsis* cell cultures occurs mainly in the endomembrane system and continues at a reduced rate after secretion. *Annals of Botany*, **130**, 703–715.

Bell E M, Lin W C, Husbands A Y, Yu L, Jaganatha V, Jablonska B, Mangeon A, Neff M M, Girke T, Springer P S. 2012. *Arabidopsis* LATERAL ORGAN BOUNDARIES negatively regulates brassinosteroid accumulation to limit growth in organ boundaries. *Proceedings of the National Academy of Sciences of the United States of America*, **109**, 21146–21151.

Bradbury P J, Zhang Z, Kroon D E, Casstevens T M, Ramdoss Y, Buckler E S. 2007. TASSEL: Software for association mapping of complex traits in diverse samples. *Bioinformatics*, **23**, 2633–2635.

Brown P H, Bellaloui N, Wimmer M A, Bassil E S, Ruiz J, Hu H, Pfeffer H, Dannel F, Römheld V. 2002. Boron in plant biology. *Plant Biology*, **4**, 205–223.

Brown P H, Shelp B J. 1997. Boron mobility in plants. *Plant and Soil*, **193**, 85–101.

Bureau M, Rast M I, Illmer J, Simon R. 2010. JAGGED LATERAL ORGAN (JLO) controls auxin dependent patterning during development of the *Arabidopsis* embryo and root. *Plant Molecular Biology*, **74**, 479–491.

Cai D, Xiao Y, Yang W, Ye W, Wang B, Younas M, Wu J, Liu K. 2014. Association mapping of six yield-related traits in rapeseed (*Brassica napus* L.). *Theoretical and Applied Genetics*, **127**, 85–96.

Camacho-Cristóbal J J, Rexach J, González-Fontes A. 2008. Boron in plants: Deficiency and toxicity. *Journal of Integrative Plant Biology*, **50**, 1247–1255.

Chen R, Deng Y, Ding Y, Guo J, Qiu J, Wang B, Wang C, Xie Y, Zhang Z, Chen J, Chen L, Chu C, He G, He Z, Huang X, Xing Y, Yang S, Xie D, Liu Y, Li J. 2022. Rice functional genomics: Decades' efforts and roads ahead. *Science China-Life Sciences*, **65**, 33–92.

Cheng F, Liu S, Wu J, Fang L, Sun S, Liu B, Li P, Hua W, Wang X. 2011. BRAD, the genetics and genomics database for *Brassica* plants. *BMC Plant Biology*, **11**, 136.

Chormova D, Messenger D J, Fry S C. 2014. Rhamnogalacturonan-II cross-linking of plant pectins *via* boron bridges occurs during polysaccharide synthesis and/or secretion. *Plant Signaling & Behavior*, **9**, e28169.

Dinka S J, Campbell M A, Demers T, Raizada M N. 2007. Predicting the size of the progeny mapping population required to positionally clone a gene. *Genetics*, **176**, 2035–2054.

Fu W, Zhao L, Qiu W, Xu X, Ding M, Lan L, Qu S, Wang S. 2024. Whole-genome resequencing identifies candidate genes and allelic variation in the MdNADP-ME promoter that regulate fruit malate and fructose contents in apple. *Plant Communicaiton*, **14**, 100973.

He M, Wang S, Zhang C, Liu L, Zhang J, Qiu S, Wang H, Yang G, Xue S, Shi L, Xu F. 2021. Genetic variation of *BnaA3.NIP5;1* expressing in the lateral root cap contributes to boron deficiency tolerance in *Brassica napus*. *PLoS Genetics*, **17**, e1009661.

He M, Zhang C, Chu L, Wang S, Shi L, Xu F. 2021. Specific and multiple-target gene silencing reveals function diversity of *BnaA2.NIP5;1* and *BnaA3.NIP5;1* in *Brassica napus*. *Plant*, *Cell & Environment*, **44**, 3184–3194.

Hu J H, Chen B Y, Zhao J, Zhang F G, Xie T, Xu K, Gao G Z, Yan G X, Li H G, Li L X, Ji G X, An H, Li H, Huang Q, Zhang M L, Wu J F, Song W L, Zhang X J, Luo Y J, Pires J C, *et al*. 2022. Genomic selection and genetic architecture of agronomic traits during modern rapeseed breeding. *Nature Genetics*, **54**, 694–704.

Hua Y, Feng Y, Zhou T, Xu F. 2017. Genome-scale mRNA transcriptomic insights into the responses of oilseed rape (*Brassica napus* L.) to varying boron availabilities. *Plant and Soil*, **416**, 205–225.

Hua Y, Zhang D, Zhou T, He M, Ding G, Shi L, Xu F. 2016a. Transcriptomics-assisted quantitative trait locus fine mapping for the rapid identification of a nodulin 26-like intrinsic protein gene regulating boron efficiency in allotetraploid rapeseed. *Plant*, *Cell & Environment*, **39**, 1601–1618.

Hua Y, Zhou T, Ding G, Yang Q, Shi L, Xu F. 2016b. Physiological, genomic and transcriptional diversity in responses to boron deficiency in rapeseed genotypes. *Journal of Experimental Botany*, **67**, 5769–5784.

Huang L, Min Y, Schiessl S, Xiong X, Jan H U, He X, Qian W, Guan C, Snowdon R J, Hua W, Guan M, Qian L. 2021. Integrative analysis of GWAS and transcriptome to reveal novel loci regulation flowering time in semi-winter rapeseed. *Plant Science*, **310**, 110980.

Kong W, An B, Zhang Y, Yang J, Li S, Sun T, Li Y. 2019. Sugar transporter proteins (STPs) in gramineae crops: Comparative analysis, phylogeny, evolution, and expression profiling. *Cells*, **8**, 560.

Körber N, Bus A, Li J, Parkin I A P, Wittkop B, Snowdon R J, Stich B. 2016. Agronomic and seed quality traits dissected by genome-wide association mapping in *Brassica napus*. *Frontiers in Plant Science*, **7**, 386.

Lin M, Islamov B, Aleliūnas A, Armonienė R, Gorash A, Meigas E, Ingver A, Tamm I, Kollist H, Strazdiņa V, Bleidere M, Brazauskas G, Lillemo M. 2024. Genome-wide association analysis identifies a consistent QTL for powdery mildew resistance on chromosome 3A in Nordic and Baltic spring wheat. *Theoretical and Applied Genetics*, **137**, 25.

Liu T, Bao C, Ban Q, Wang C, Hu T, Wang J. 2022. Genome-wide identification of sugar transporter gene family in *Brassicaceae* crops and an expression analysis in the radish. *BMC Plant Biology*, **22**, 245.

Livak K J, Schmittgen T D. 2001. Analysis of relative gene expression data using real-time quantitative PCR and the $2^{-\Delta\Delta CT}$ method.

Methods, **25**, 402–408.
Lu K, Peng L, Zhang C, Lu J, Yang B, Xiao Z, Liang Y, Xu X, Qu C, Zhang K, Liu L, Zhu Q, Fu M, Yuan X, Li J. 2017. Genome-wide association and transcriptome analyses reveal candidate genes underlying yield-determining traits in *Brassica napu*s. *Frontiers in Plant Science*, **8**, 206.
Lu K, Wei L, Li X, Wang Y, Wu J, Liu M, Zhang C, Chen Z, Xiao Z, Jian H, Cheng F, Zhang K, Du H, Cheng X, Qu C, Qian W, Liu L, Wang R, Zou Q, Ying J, *et al.* 2019. Whole-genome resequencing reveals *Brassica napus* origin and genetic loci involved in its improvement. *Nature Communication*, **10**, 1154.
Lu K, Xiao Z, Jian H, Peng L, Qu C, Fu M, He B, Tie L, Liang Y, Xu X, Li J. 2016. A combination of genome-wide association and transcriptome analysis reveals candidate genes controlling harvest index-related traits in *Brassica napus*. *Scientific Reports*, **6**, 36452.
Naito T, Yamashino T, Kiba T, Koizumi N, Kojima M, Sakakibara H, Mizuno T. 2007. A link between cytokinin and *ASL9* (*ASYMMETRIC LEAVES 2 LIKE 9*) that belongs to the *AS2/LOB* (*LATERAL ORGAN BOUNDARIES*) family genes in *Arabidopsis thaliana*. *Bioscience*, *Biotechnology*, *and Biochemistry*, **71**, 1269–1278.
Onuh A F, Miwa K. 2021. Regulation, diversity and evolution of boron transporters in plants. *Plant and Cell Physiology*, **62**, 590–599.
Pal L, Sandhu S K, Bhatia D, Sethi S. 2021. Genome-wide association study for candidate genes controlling seed yield and its components in rapeseed (*Brassica napus* L.). *Physiology and Molecular Biology of Plants*, **27**, 1933–1951.
Piepho H P, Büchse A, Emrich K. 2003. A Hitchhiker's guide to mixed models for randomized experiments. *Journal of Agronomy and Crop Science*, **189**, 310–322.
Prince S J, Valliyodan B, Ye H, Yang M, Tai S, Hu W, Murphy M, Durnell L A, Song L, Joshi T, Liu Y, Van de Velde J, Vandepoele K, Grover Shannon J, Nguyen H T. 2019. Understanding genetic control of root system architecture in soybean: Insights into the genetic basis of lateral root number. *Plant*, *Cell & Environment*, **42**, 212–229.
Qian M, Fan Y, Li Y, Liu M, Sun W, Duan H, Yu M, Chang W, Niu Y, Li X, Liang Y, Qu C, Li J, Lu K. 2021. Genome-wide association study and transcriptome comparison reveal novel QTL and candidate genes that control petal size in rapeseed. *Journal of Experimental Botany*, **72**, 3597–3610.
Schoenaers S, Lee H K, Gonneau M, Faucher E, Levasseur T, Akary E, Claeijs N, Moussu S, Broyart C, Balcerowicz D, AbdElgawad H, Bassi A, Damineli D S C, Costa A, Feijó J A, Moreau C, Bonnin E, Cathala B, Santiago J, Höfte H, *et al.* 2024. Rapid alkalinization factor 22 has a structural and signaling role in root hair cell wall assembly. *Nature Plants*, **10**, 494–511.
Scholz-Starke J, Büttner M, Sauer N. 2003. AtSTP6, a new pollen-specific H^+-monosaccharide symporter from *Arabidopsis*. *Plant Physiology*, **131**, 70–77.
Shen X, Song S, Li C, Zhang J. 2022. Synonymous mutations in representative yeast genes are mostly strongly non-neutral. *Nature*, **606**, 725–731.
Takano J, Miwa K, Yuan L, von Wirén N, Fujiwara T. 2005. Endocytosis and degradation of BOR1, a boron transporter of *Arabidopsis thaliana*, regulated by boron availability. *Proceedings of the National Academy of Sciences of the United States of America*, **102**, 12276–12281.
Takano J, Noguchi K, Yasumori M, Kobayashi M, Gajdos Z, Miwa K, Hayashi H, Yoneyama T, Fujiwara T. 2002. *Arabidopsis* boron transporter for xylem loading. *Nature*, **420**, 337–340.
Takano J, Tanaka M, Toyoda A, Miwa K, Kasai K, Fuji K, Onouchi H, Naito S, Fujiwara T. 2010. Polar localization and degradation of *Arabidopsis* boron transporters through distinct trafficking pathways. *Proceedings of the National Academy of Sciences of the United States of America*, **107**, 5220–5225.
Takano J, Wada M, Ludewig U, Schaaf G, von Wirén N, Fujiwara T. 2006. The *Arabidopsis* major intrinsic protein NIP5;1 is essential for efficient boron uptake and plant development under boron limitation. *The Plant Cell*, **18**, 1498–1509.
Tan H, Xiang X, Tang J, Wang X. 2016. Nutritional functions of the funiculus in *Brassica napus* seed maturation revealed by transcriptome and dynamic metabolite profile analyses. *Physiology and Molecular Biology of Plants*, **92**, 539–553.
Tanaka M, Fujiwara T. 2008. Physiological roles and transport mechanisms of boron: Perspectives from plants. *Pflügers Archiv-European Journal of Physiology*, **456**, 671–677.
Tanaka M, Wallace I S, Takano J, Roberts D M, Fujiwara T. 2008. NIP6;1 is a boric acid channel for preferential transport of boron to growing shoot tissues in *Arabidopsis*. *The Plant Cell*, **20**, 2860–2875.
Tang S, Zhao H, Lu S, Yu L, Zhang G, Zhang Y, Yang QY, Zhou Y, Wang X, Ma W, Xie W, Guo L. 2021. Genome- and transcriptome-wide association studies provide insights into the genetic basis of natural variation of seed oil content in *Brassica napus*. *Molecular Plant*, **14**, 470–487.
Thatcher L F, Powell J J, Aitken E A B, Kazan K, Manners J M. 2012. The lateral organ boundaries domain transcription factor LBD20 functions in Fusarium wilt susceptibility and jasmonate signaling in *Arabidopsis*. *Plant Physiology*, **160**, 407–418.
U.S. Department of Agriculture (USDA), Economic Research Service (ERS). 2024. *Oil Crops Yearbook*. [2024-3-25]. https://www.ers.usda.gov/data-products/oil-crops-yearbook/
Wang Y, Shi L, Cao X, Xu F. 2007. Boron nutrition and boron application in crops. In: Xu F, Goldbach H E, Brown P H, eds., *Advances in Plant and Animal Boron Nutrition*, *Proceedings of the 3rd International Symposium on All Aspects of Plant and Animal Boron Nutrition*. Springer Publishing, Dordrecht, Netherlands. pp. 93–101.
Warington K. 1923. The effect of boric acid and borax on the broad bean and certain other plants. *Annals of Botany*, **os-37**, 629–672.
Wu D, Liang Z, Yan T, Xu Y, Xuan L, Tang J, Zhou G, Lohwasser U, Hua S, Wang H, Chen X, Wang Q, Zhu L, Maodzeka A, Hussain N, Li Z, Li X, Shamsi I H, Jilani G, Wu L, *et al.* 2019. Whole-genome resequencing of a worldwide collection of rapeseed accessions reveals the genetic basis of ecotype divergence. *Molecular Plant*, **12**, 30–43.
Xiao Y, Liu H, Wu L, Warburton M, Yan J. 2017. Genome-wide association studies in maize: Praise and stargaze. *Molecular Plant*, **10**, 359–374.
Xu F, Wang Y, Meng J. 2001. Mapping boron efficiency gene(s) in *Brassica napus* using RFLP and AFLP markers. *Plant Breeding*, **120**, 319–324.
Xu F, Wang Y, Ying W, Meng J. 2002. Inheritance of boron nutrition efficiency in *Brassica napus*. *Journal of Plant Nutrition*, **25**, 901–912.
Yuan P, Liu H, Wang X, Hammond J P, Shi L. 2023. Genome-wide association study reveals candidate genes controlling root system architecture under low phosphorus supply at seedling stage in *Brassica napus*. *Molecular Breeding*, **43**, 63.
Zhang C, Dong S, Xu J, He W, Yang T. 2019. PopLDdecay: A fast and effective tool for linkage disequilibrium decay analysis based on variant call format files. *Bioinformatics*, **35**, 1786–1788.
Zhang C, He M, Jiang Z, Liu L, Pu J, Zhang W, Wang S, Xu F. 2022. The xyloglucan endotransglucosylase/hydrolase gene XTH22/TCH4 regulates plant growth by disrupting the cell wall homeostasis in *Arabidopsis* under boron deficiency. *International Journal of Molecular Sciences*, **23**, 1250.
Zhang D, Hua Y, Wang X, Zhao H, Shi L, Xu F. 2014a. A high-density genetic map identifies a novel major QTL for boron efficiency in oilseed rape (*Brassica napus* L.). *PLoS ONE*, **9**, e112089.
Zhang D, Zhao H, Shi L, Xu F. 2014b. Physiological and genetic responses to boron deficiency in *Brassica napus*: A review. *Soil Science and Plant Nutrition*, **60**, 304–313.
Zhao H, Shi L, Duan X, Xu F, Wang Y, Meng J. 2008. Mapping and validation of chromosome regions conferring a new boron-efficient locus in *Brassica napus*. *Molecular Breeding*, **22**, 495–506.
Zhao Z, Wu L, Nian F, Ding G, Shi T, Zhang D, Shi L, Xu F, Meng J. 2012. Dissecting quantitative trait loci for boron efficiency across multiple environments in *Brassica napus*. *PLoS ONE*, **7**, e45215.
Zhou T, Hua Y, Huang Y, Ding G, Shi L, Xu F. 2016. Physiological and transcriptional analyses reveal differential phytohormone responses to boron deficiency in *Brassica napus* genotypes. *Frontiers in Plant Science*, **7**, 221.

Executive Editor-in-Chief Xueyong Zhang
Managing Editor Ning Wang